Preparation of multiferroic Co substituted BiFeO$_3$ with enhanced coercive force and its application in sorption removal of dye molecules from aqueous solution

Lirong Luo [a], Kai Shen [a,*], Qingyu Xu [b,c,*], Qin Zhou [d], Wei Wei [a], M.A. Gondal [e]

[a] College of Materials Science and Technology, Nanjing University of Aeronautics and Astronautics, Nanjing 210016, China
[b] Department of Physics, Southeast University, Nanjing 211189, China
[c] Key Laboratory of MEMS of the Ministry of Education, Southeast University, Nanjing 210096, China
[d] State Key Laboratory of Environmental Aquatic Chemistry, Research Center for Eco-environmental Sciences, Chinese Academy of Sciences, Beijing 100085, China
[e] Physics Department and Center of Excellence in Nanotechnology, King Fahd University of Petroleum and Minerals, Dhahran 31261, Saudi Arabia

ARTICLE INFO

ABSTRACT

Multiferroic Co substituted BiFeO$_3$ (BiFe$_{0.95}$Co$_{0.05}$O$_3$) compound was synthesized by complex sol–gel method and its potential application as an efficient magnetic adsorbent in sorption removal of organic contaminants (like Rhodamine B as a model compound) was investigated. The XRD, Raman, and PPMS measurement revealed that Co substituted BiFeO$_3$ enhances magnetic properties dramatically at room temperature without inducing any impurity phase. This aspect is very useful for many applications of Co substituted BiFeO$_3$ especially in magnetic separation of this catalyst after its utilization in water purification. The adsorption kinetics, isotherm, thermodynamic as well as the possible sorption mechanism was studied through batch experiments. Almost no negative effect on the sorption performance (i.e. the sorption rate and saturated sorption capacity) was found after substitution of Co in BiFeO$_3$. In addition, this substitution give rise to much higher coercive force of BiFe$_{0.95}$Co$_{0.05}$O$_3$ which can be recycled more easily by magnetic separation technology.

1. Introduction

Nowadays, organic pollutants like dyes which have severe and chronic effects on living organisms have been considered major cause of water contamination [1,2]. Rhodamine B (RhB) is widely used as a colorant in textile industries and is harmful to human beings and animals which could yield potentially carcinogenic aromatic amines under natural reductive anaerobic degradation [3]. So far, many efforts have devoted to remove RhB from aqueous solution by developing new technologies and materials to solve this problem. Based on the results, adsorption process has the advantage of low generation of residues and the possibility of reuse of the adsorbent. Due to these factors, adsorption process has been recognized as an efficient and economic method [4].

Multiferroic materials which exhibit unique ferroic properties such as ferroelectric, ferromagnetic and ferroelastic in a single phase have drawn great attention driven by their potential applications for new electronic devices and intriguing fundamental physics [5,6]. Perovskite-type BiFeO$_3$ with ferroelectric and antifer-

romagnetic orderings above room-temperature ($T_C \sim 1103$ K, $T_N \sim 643$ K), make it one of the most promising candidate for practical applications [7]. However, weak macroscopic magnetism attributing to canted G-type antiferromagnetic spin structure limited its advancement [8]. Comparing with other methods, ion substitution is an effective mean to improve the multiferroic property. Our previous achievements [9–11] clearly demonstrated that the Co substituted at Fe site could improve room temperature magnetism significantly attributing to the suppression of the spiral spin configuration, which suggests its good application in magnetic separation especially with the concentration of 5% [12]. In terms of environmental remediation, BiFeO$_3$ is being applied as photocatalyst owning to its small band gap and has been studied intensively. However to the best of our knowledge, little work has been focused on adsorption performance of BiFeO$_3$ [13,14].

In this paper, BiFeO$_3$ and BiFe$_{0.95}$Co$_{0.05}$O$_3$ ceramics were synthesized by a tartaric acid modified sol–gel method. The microstructure as well as the magnetic properties of as-prepared multiferroic oxides was characterized by means of X-ray diffraction (XRD) patterns, Raman spectra and physical property measurements (PPMS). The sorption kinetics, isotherm and thermodynamics were investigated by selecting Rhodamine B (RhB) and multiferroic BiFe$_{0.95}$Co$_{0.05}$O$_3$ as a sorbate and sorbent, respectively. Furthermore the possible sorption mechanism has been discussed based on the static-electric adsorption process.

* Corresponding authors. Addresses: College of Materials Science and Technology, Nanjing University of Aeronautics and Astronautics, Nanjing 210016, China (K. Shen), Department of Physics, Southeast University, Nanjing 211189, China (Q. Xu).
E-mail addresses: shenkai84@nuaa.edu.cn (K. Shen), xuqingyu@seu.edu.cn (Q. Xu).

2. Experimental

2.1. Preparation of BiFeO₃ and BiFe₀.₉₅Co₀.₀₅O₃ powder

$BiFeO_3$ and $BiFe_{0.95}Co_{0.05}O_3$ ceramics were prepared by a tartaric acid modified sol–gel method. Raw materials of $Bi(NO_3)_3 \cdot 5H_2O$, $Fe(NO_3)_3 \cdot 9H_2O$ and $Co(NO_3)_2 \cdot 6H_2O$ of analytical-grade were dissolved in diluted HNO_3 in proper stoichiometric proportions. Tartaric acid in 1:1 M ratio with respect to metal nitrates was added to the solution, which was heated in 150 °C to form xero gel. After grinded thoroughly, the powder was sintered at 600 °C for 2 h. The obtained $BiFe_{0.95}Co_{0.05}O_3$ sample was leached in diluted far about half an hour, and washed in deionized water repeatedly to remove the trace amounts of impurity.

2.2. Characterization

The crystal structure of both samples was characterized by X-ray diffraction (XRD) with Cu Kα radiation (Rigaku Smartlab). The magnetic properties were investigated by Physical Property Measurement System (PPMS-9, Quantum Design) at room temperature. Raman measurements were carried out on a Horiba Jobin Yvon LabRAM HR 800 micro-Raman spectrometer with 785 nm excitation source under ambient air conditions at room temperature. The zeta potentials as-prepared $BiFe_{0.95}Co_{0.05}O_3$ at different pHs were determined by a zeta potential instrument (Malvern, Great Britain).

2.3. Batch sorption evaluation

All the sorption experiments were conducted under dark conditions in a thermostatic stirrer equipped with water bath. The stirring speed of the magnetic bar was measured at around 150 rpm. The pH of solution was adjusted by diluted HCl or NaOH aqueous solution. After sorption process for certain period, the residual solution without adsorbent was separated through centrifugation. The concentration variation of RhB was monitored by UV–Vis spectrometer (HITACHI U-3900) at wavelength of 554 nm. All the experiments were conducted at least twice and took the average of the results.

3. Results and discussion

Fig. 1 depicts the XRD patterns of $BiFeO_3$ and $BiFe_{0.95}Co_{0.05}O_3$. All peaks of $BiFeO_3$ shows the rhombohedral perovskite structure with the space group of R3c, except a small peak of $BiFeO_3$ marked by ∗ which can be attributed to the small amount of impurity of $Bi_2Fe_4O_9$ [15]. After washed by diluted HNO_3 and deioned water, the $BiFe_{0.95}Co_{0.05}O_3$ does not show any impurity phase. The peaks of 5% Co doping at Fe site are similar to pure $BiFeO_3$ indicating that no obvious structure transformation was induced. Magnetic hysteresis loops of both samples as illustrated in Fig. 2 were measured at 300 K by PPMS. The linear curve was observed for $BiFeO_3$ which is in accord with the antiferromagnetic properties. The remnant magnetization and coercivity of $BiFe_{0.95}Co_{0.05}O_3$ ($M_r = 0.02$ emu/g; $H_c = 710.21$ Oe) are enhanced significantly by contrast with pure $BiFeO_3$ ($M_r = 0.001$ emu/g; $H_c = 80$ Oe). It is worth noticing that the 5% Co doping at Fe site shows significant improvement in mag-
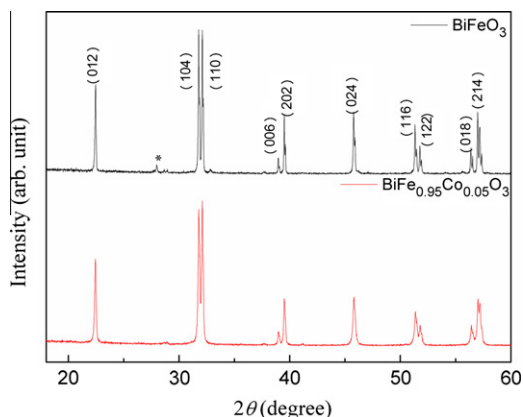
netic properties without inducing any impurity phase. The improved magnetization effect suggests the application of this material in magnetic separation.

The details of structure evolution induced by Co substituted at Fe site were further studied by Raman spectra (Fig. 3). Theoretically, 13 Raman active modes ($4A_1 + 9E$) are expected for the rhombohedral $BiFeO_3$ [16]. However, with the temperature increasing to higher values, the intensity of many major peaks decreased and higher wavenumber peaks were broadened and merged into single broadened peak and even disappeared [17]. So, only three A_1 modes (A_1-1, A_1-2, A_1-3) could be noticed clearly for both samples at room temperature. It can be noticed that the A_1-1 mode of $BiFe_{0.95}Co_{0.05}O_3$ shifted to lower frequency and the intensity of A_1-2 mode decreased apparently comparing with $BiFeO_3$. The shift of A_1-1 mode which is associated with the vibration of Bi–O bond showed that Co doping produced more structural distortion on Fe site [9,18]. The decrement of A_1-2 mode which could be associated with magnetic transition representing spin reorientation indicates the change in magnetic property [19].

The kinetic curves of adsorption of $BiFeO_3$ and $BiFe_{0.95}Co_{0.05}O_3$ measured at 293 K and 303 K are demonstrated in Fig. 4. The Pseudo-first-order dynamic model and pseudo-second-order kinetic model were carried out to fit this data.

Pseudo-first-order dynamic model:

$$\ln(q_e - q_t) = \ln(q_e) - k_1 t \quad (1)$$

Pseudo-second-order kinetic model:

$$\frac{t}{q_t} = \frac{1}{k_2 q_e^2} + \frac{t}{q_e} \quad (2)$$

where q_t (mg g^{-1}) and q_e (mg g^{-1}) are the adsorption capacity at specific contact time and equilibrium; k_1 (h^{-1}) and k_2 (g mg^{-1} h^{-1}) are the adsorption constants. The related coupling parameters were listed in Table 1. According to the correlation coefficients, the experimental data fits very well to the pseudo-second-order model ($r^2 > 0.94$) better than pseudo-first-order dynamic model which indicates that sorption rate is possibly controlled by chemical sorption and the sorption capacity is proportional to the number of active sites on the sorbent [20]. All the adsorption process reached to equilibrium in 2 h. It is obvious that the substitution of cobalt in $BiFeO_3$ cannot decrease the sorption rate but contrary improve the sorption rate to a certain extent. With the temperature decrease from 303 K to 293 K, the adsorption constants of both samples decreased from 43.579 g mg^{-1} h^{-1} and 254.632 g mg^{-1} h^{-1} to 2.183 g mg^{-1} h^{-1} and 6.371 g mg^{-1} h^{-1}, while the equilibrium adsorption amount (q_e) increased from 0.185 mg g^{-1} and 0.216 mg g^{-1} to 0.516 mg g^{-1} and 0.537 mg g^{-1}. This behavior could be due to the competition result of the molecular diffusion
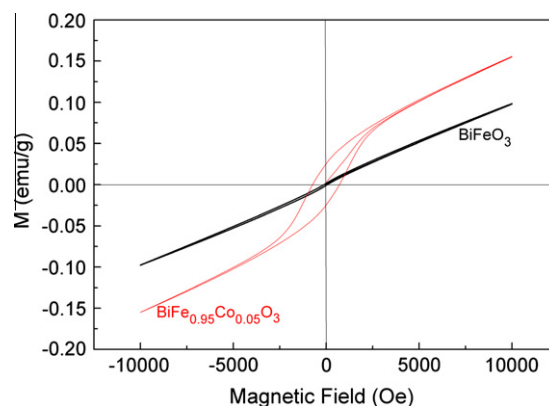

Fig. 1. XRD patterns of $BiFeO_3$ and $BiFe_{0.95}Co_{0.05}O_3$. The peak marked by ∗ indicates the impurity phase of $Bi_2Fe_4O_9$.

Fig. 2. M–H curves of $BiFeO_3$ and $BiFe_{0.95}Co_{0.05}O_3$ measured at 300 K.
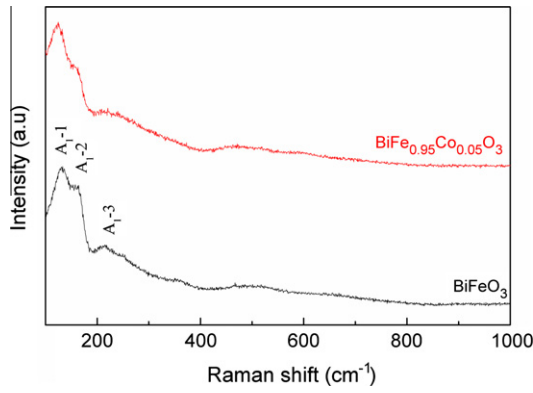
Fig. 3. Raman spectra of $BiFeO_3$ and $BiFe_{0.95}Co_{0.05}O_3$ measured at room temperature.
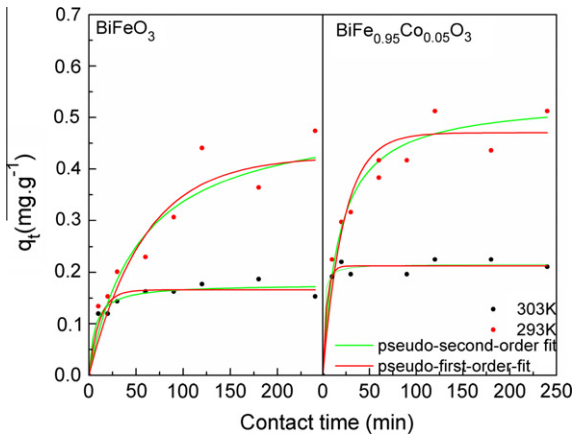

Fig. 4. Dependence of adsorption kinetic of RhB over $BiFeO_3$ and $BiFe_{0.95}Co_{0.05}O_3$ at different adsorption temperatures.

Table 1
Parameters of pseudo-second-order and pseudo-first-order fit of $BiFeO_3$ and $BiFe_{0.95}$-$Co_{0.05}O_3$ toward removal of RhB measured at 293 K and 303 K respectively.

	Pseudo-first-order model			Pseudo-second-order model		
	q_e (mg g^{-1})	k_1 (h^{-1})	r^2	q_e (mg g^{-1})	k_2 (g mg^{-1} h^{-1})	r^2
$BiFeO_3$ (293 K)	0.425	1.02	0.91	0.516	2.183	0.940
$BiFeO_3$ (303 K)	0.167	5.419	0.937	0.185	43.579	0.976
$BiFe_{0.95}Co_{0.05}O_3$ (293 K)	0.470	2.680	0.933	0.537	6.371	0.971
$BiFe_{0.95}Co_{0.05}O_3$ (303 K)	0.213	14.331	0.977	0.216	254.632	0.976

and adsorption. At low temperature, the adsorption holds the advantage and molecular diffusion velocity is low, and vice versa.

The thermodynamic parameters like Gibbs free energy, enthalpy and entropy are calculated using the following equations:

$$\Delta G_{abs} = -RT\ln K_{abs} \tag{3}$$

$$\Delta G_{abs} = \Delta H_{abs} - T\Delta S_{abs} \tag{4}$$

where K_{abs} is the equilibrium constant at different temperature defined by $(C_o - C_e)/C_e$; R is ideal gas constant. The obtained values of the thermodynamic parameter are listed in Table 2. The free energy obtained are all above zero, which indicates that the adsorption of RhB on both samples are not a spontaneous process and may be

Table 2
Thermodynamic parameters of Rhodamine B adsorption on $BiFeO_3$ and $BiFe_{0.95}Co_{0.05}O_3$.

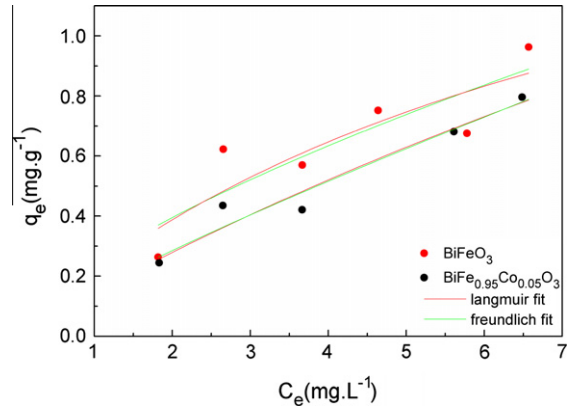|	ΔG^o (kJ mol^{-1})	ΔH^o (kJ mol^{-1})	ΔS^o (J K^{-1} mol^{-1})
$BiFeO_3$ (293 K)	0.73	−5.13	−0.02
$BiFeO_3$ (303 K)	0.93		
$BiFe_{0.95}Co_{0.05}O_3$ (293 K)	0.62	−6.412	−0.024
$BiFe_{0.95}Co_{0.05}O_3$ (303 K)	0.86		

Fig. 5. Adsorption isotherms of RhB using $BiFeO_3$ and $BiFe_{0.95}Co_{0.05}O_3$ as adsorbent.

the energy gain from other source [21] and the enthalpy (ΔH^o) of small negative value shows that this progress is endothermic.

The isothermal adsorption data depicted in Fig. 5 was fitted by Langmuir and Freundlich model. The Langmuir equation which is an empirical formula with the assumption of monolayer coverage can be expressed as:

$$q_e = \frac{q_m k_L c_e}{(1 + k_L c_e)} \tag{5}$$

The Freundlich equation can be written as following:

$$q_e = K_F C_e^{1/n} \tag{6}$$

where q_e (mg g^{-1}) is the saturated adsorption capacity; C_e (mg L^{-1}) is the equilibrium concentration in RhB solution; q_m (mg g^{-1}) is the theoretical monolayer capacity; k_L (L mg^{-1}) is Langmuir constant. k_F (mg$^{1-1/n}$ L$^{1/n}$ g^{-1}) and n are Freundlich constants, representing the sorption capacity and sorption intensity respectively. As listed in Table 3, the correlation coefficients of Langmuir and Freundlich fit are similar which cannot conclude that which fit is better. However comparable monolayer capacities q_m (mg g^{-1}) of $BiFeO_3$ (1.951 mg g^{-1}) and after cobalt substitution (3.84 mg g^{-1}) can be found by non-linear fitting, suggesting that the substitution of cobalt in $BiFeO_3$ does not affect the sorption capacity negatively.

In order to further reveal the possible sorption mechanism, the saturated adsorption capacity of $BiFe_{0.95}Co_{0.05}O_3$ as function of pH was investigated. It is obvious that the adsorption capacity significantly increases from 0.11 mg g^{-1} to 2.15 mg g^{-1} when the pH decreases from 9.98 to 1.69, suggesting that electrostatic interaction should be involved in the sorption process. The zeta potential of $BiFe_{0.95}Co_{0.05}O_3$ was measured and is depicted in Fig. 6. The isoelectric point of $BiFe_{0.95}Co_{0.05}O_3$ is around 5.2, which is almost the same with the $BiFeO_3$ oxides [13]. Under lower pH conditions (pH < 5.2), the electrostatic interaction might be occurred between the positive charged surface of $BiFe_{0.95}Co_{0.05}O_3$ and the negative charged carboxyl groups. However, the sorption still can be found in basic conditions, even though the sorption capacity is much smaller, indicating that the inter-molecular interaction might be

Table 3
Parameters of Langmuir and Freundlich fit of BiFeO$_3$ and BiFe$_{0.95}$Co$_{0.05}$O$_3$ toward removal of RhB measured at 298 K.

	Langmuir model			Freundlich model		
	q_m (mg g^{-1})	k_L (L mg^{-1})	r^2	k_F (mg$^{1-1/n}$ L$^{1/n}$ g^{-1})	n	r^2
BiFeO$_3$	1.951	0.124	0.779	0.246	1.456	0.773
BiFe$_{0.95}$Co$_{0.05}$O$_3$	3.843	0.039	0.950	0.158	1.170	0.952
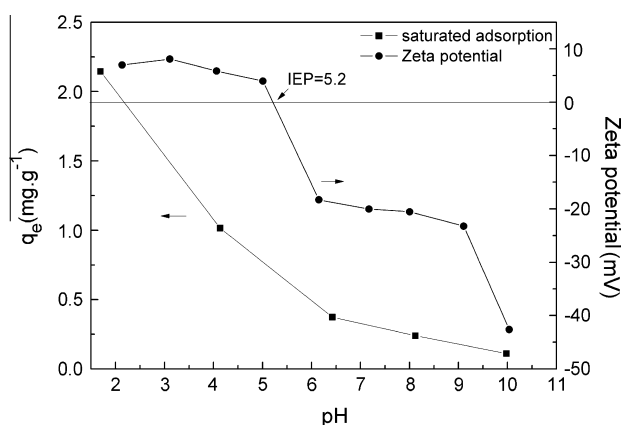
Fig. 6. Zeta potential and the saturated adsorption of RhB onto BiFe$_{0.95}$Co$_{0.05}$O$_3$ as function of pH measured at room temperature.

Fig. 7. Magnetic separability of as-prepared BiFe$_{0.95}$Co$_{0.05}$O$_3$ and BiFeO$_3$. (The adsorbent can be effectively attracted by the magnet and accumulated in the left one.)

possibly involved, such as the chemical binding of carboxylic group in RhB on the surface of oxides by monodentate (ester-like) linkage [22]. On the other hand, the fitting results by pseudo-second-order model which assumes the sorption capacity is proportional to the number of active sites on the sorbent, also indicates the probable chemical sorption mechanism. In the meantime, it is worth noticing that the electrostatic interaction between negative charged BiFe$_{0.95}$Co$_{0.05}$O$_3$ and positively charged diethylamine function group also could possibly be occurred as well [23].

The magnetic separation effect of BiFeO$_3$ (right) and BiFe$_{0.95}$Co$_{0.05}$O$_3$ (left) after adsorption have been detected. 0.025 g adsorbent added to 10 ml RhB solution (7 ppm). The pH of solution was adjusted to 2 using HCl solution. After adsorption for 24 h, the permanent magnet of 0.4 T was applied to characterize the magnetic response. The distance between the bottle and magnet was 1.6 cm. Apparently the BiFe$_{0.95}$Co$_{0.05}$O$_3$ shows better magnetic response, which suggests its application in magnetic separation process (see Fig. 7).

4. Conclusions

In this work, BiFeO$_3$ and BiFe$_{0.95}$Co$_{0.05}$O$_3$ were prepared by a complex sol–gel method by using tartaric acid as ligand. This study demonstrated that the Co doping at Fe site with 5% concentration improved the magnetism significantly (M_r = 0.02 emu/g; H_c = 710.21 Oe) as compared with pure BiFeO$_3$ (M_r = 0.001 emu/g; H_c = 80 Oe), which suggests its possible application in efficient magnetic separation of the powder adsorbent. The batch sorption experiments clearly revealed that BiFe$_{0.95}$Co$_{0.05}$O$_3$ with enhanced coercive force exhibits comparable sorption performance in terms of sorption rate as well as saturated sorption capacity. Furthermore our investigation demonstrated that the electrostatic interaction might be of vital importance during the sorption process but the inter-molecular interaction cannot be neglected as well.

References

[1] J.X. Yu, R. Chi, Y.F. Zhang, Z.G. Xu, C.Q. Xiao, J. Guo, Bioresource. Technol. 110 (2012) 160.
[2] B.H. Hameed, A.A. Ahmad, N. Aziz, Chem. Eng. J. 133 (2007) 195.
[3] J.F. Luan, M. Li, K. Ma, Y.M. Li, Z.G. Zou, Chem. Eng. J. 167 (2011) 162.
[4] R. Jain, M. Mathura, S. Sikarwar, A. Mittal, J. Environ. Manage. 85 (2007) 956.
[5] S.T. Zhang, Y. Zhang, M.H. Lu, C.L. Du, Y.F. Chen, Appl. Phys. Lett. 88 (2006) 162901.
[6] S.T. Zhang, M.H. Lu, D. Wu, Y.F. Chen, N.B. Ming, Appl. Phys. Lett. 87 (2005) 262907.
[7] Z.X. Cheng, A.H. Li, X.L. Wang, S.X. Dou, K. Ozawa, H. Kimura, S.J. Zhang, T.R. Shrout, J. Appl. Phys. 103 (2008) 07E507.
[8] H. Béa, M. Bibes, S. Petit, J. Kreisel, A. Barthélémy, Philos. Mag. Lett. 87 (2007) 165.
[9] X.H. Zheng, Q.Y. Xu, Z. Wen, X.Z. Lang, D. Wu, T. Qiu, M.X. Xu, J. Alloy, Compd. 499 (2010) 108.
[10] Q.Y. Xu, H.F. Zai, D. Wu, T. Qiu, M.X. Xu, Appl. Phys. Lett. 95 (2009) 112510.
[11] Q.Y. Xu, S.Q. Zhou, D. Wu, M. Uhlarz, Y.K. Tang, K. Potzger, M.X. Xu, H. Schmidt, J. Appl. Phys. 107 (2010) 093920.
[12] Y.G. Wang, G. Xu, L.L. Yang, Z.H. Ren, X. Wei, W.J. Weng, P.Y. Du, G. Shen, G.R. Han, Mater. Lett. 62 (2008) 3806.
[13] J. Zhang, M.A. Gondal, W. Wei, T.N. Zhang, Q.Y. Xu, K. Shen, J. Alloy, Compd. 530 (2012) 107.
[14] F. Gao, X. Chen, K. Yin, S. Dong, Z. Ren, F. Yuan, T. Yu, Z. Zou, J.M. Liu, Adv. Mater. 19 (2007) 2889–2892.
[15] J.J. Ge, X.B. Xue, G.F. Cheng, Y. Mang, B. You, W. Zhang, J. Magn. Magn. Mater. 324 (2012) 200.
[16] N.V. Minh, D.V. Thang, J. Alloy, Compd. 505 (2010) 619.
[17] D. Rout, K.S. Moon, S.J.L. Kang, J. Raman, Spectrosc. 40 (2009) 618.
[18] T.J. Park, G.C. Papaefthymiou, A.J. Viescas, A.R. Moodenbaugh, S.S. Wong, Nano. Lett. 7 (2007) 766.
[19] M.M. Shirolkar, R. Das, T. Maity, P. Poddar, S.K. Kulkarni, J. Phys. Chem. C. 116 (2012) 19503.
[20] Q. Yu, R.Q. Zhang, S.B. Deng, J. Huang, G. Yu, Water. Res. 43 (2009) 1150.
[21] A. Ozcan, E.M. Oncu, A.S. Ozcan, Colloids. Surf. A: Physicochem. Eng. Aspect 277 (2006) 73.
[22] Q. Wang, C.C. Chen, D. Zhao, W.H. Ma, J.C. Zhao, Langmuir. 24 (2008) 7338.
[23] K. Yu, S.G. Yang, H. He, C. Sun, C.G. Gu, Y.M. Ju, J. Phys. Chem. A. 113 (2009) 10024.